# Yersinia Protein Kinase YopO Is Activated by A Novel G-actin Binding Process*⑤

**Claudia Trasak[‡1], Gerhardt Zenner[‡1], Annette Vogel[§], Gülnihal Yüksekdag[¶], René Rost[§], Ilka Haase[||], Markus Fischer[||], Lars Israel[**], Axel Imhof[**], Stefan Linder[‡‡], Michael Schleicher[§], and Martin Aepfelbacher[‡2]**

From the [‡]Institut für Medizinische Mikrobiologie, Virologie, und Hygiene, Universitätsklinikum Eppendorf, Martinistrasse 52, 20246 Hamburg, Germany, [§]Adolf Butenandt Institut/Zellbiologie, Ludwig-Maximilians-Universität München, Schillerstrasse 42, 80336 München, Germany, [¶]Max von Pettenkofer Institut für Medizinische Mikrobiologie, Ludwig-Maximilians-Universität München, Pettenkoferstrasse 9a, 80336 München, Germany, [||]Institut für Organische Chemie und Biochemie, Technische Universität München, Lichtenbergstrasse 4, 85747 Garching, Germany, and [**]Protein Labor, Ludwig-Maximilians-Universität München, Schillerstrasse 42, 80336 München, Germany, and [‡‡]Institut für Prophylaxe der Kreislaufkrankheiten, Ludwig-Maximilians-Universität München, Pettenkoferstrasse 9, 80336 München, Germany

Pathogenic bacteria of the genus *Yersinia* employ a type III secretion system to inject effector proteins (Yops) into host cells. The Yops down-regulate host cell functions through unique biochemical activities. YopO, a serine/threonine kinase required for *Yersinia* virulence, is activated by host cell actin via an unknown process. Here we show that YopO kinase is activated by formation of a 1:1 complex with monomeric (G) actin but is unresponsive to filamentous (F) actin. Two separate G-actin binding sites, one in the N-terminal kinase region (amino acids 89–440) and one in the C-terminal guanine nucleotide dissociation inhibitor-like region (amino acids 441–729) of YopO, were identified. Actin binding to both of these sites was necessary for effective autophosphorylation of YopO on amino acids Ser-90 and Ser-95. A S90A/S95A YopO mutant was strongly reduced in substrate phosphorylation, suggesting that autophosphorylation activates YopO kinase activity. In cells the kinase activity of YopO regulated rounding/arborization and was specifically required for inhibition of *Yersinia* YadA-dependent phagocytosis. Thus, YopO kinase is activated by a novel G-actin binding process, and this appears to be crucial for its anti-host cell functions.

Assembly of filamentous (F)[3]-actin from monomeric (G)-actin drives cell motility, cytokinesis, and phagocytosis (1). Vesicle transport and intracellular movement of pathogenic bacteria are also dependent on actin polymerization (2, 3). The turnover of actin filaments and their organization into complex structures is controlled by a plethora of actin-binding proteins, which often are regulated by specific signal transduction pathways (4). Besides governing motile cellular processes, actin has been recognized as an important cofactor for regulators of gene transcription and cell proliferation (5). The myocardin-related serum response factor (SRF) coactivator (MAL) accumulates in the nucleus dependent upon G-actin binding and activates transcription of SRF. It has been speculated that G-actin binding activates MAL for nuclear translocation (6). A recent report suggested that actin associates with RNA polymerase I in the nucleus and in cooperation with nuclear myosin I supports transcription (7). Furthermore, c-Abl tyrosine kinase, which is involved in cell responses to DNA damage and apoptosis signaling, becomes inhibited upon interaction with F-actin (8). Hence, a number of crucial cellular regulators are controlled by G- or F-actin, but the biochemical basis for this has not been determined.

Pathogenic *Yersinia* species encompassing *Yersinia enterocolitica*, *Yersinia pseudotuberculosis*, and *Yersinia pestis* employ a type III secretion system to translocate six effector proteins (<u>Y</u>ersinia <u>o</u>uter <u>p</u>roteins, Yops) into target cells (9). Interestingly, at least four of these Yop effectors, namely YopE, -T, -H, and -O, impinge on the actin cytoskeleton (10–15). YopO from *Y. enterocolitica* (YpkA in *Y. pseudotuberculosis*) is a serine/threonine kinase that disrupts F-actin structures in host cells, causes cell rounding, and contributes to antiphagocytosis of yersiniae (16–18). YopO associates with the Rho GTP-binding proteins RhoA and Rac via a region showing homology to guanine nucleotide dissociation inhibitors (GDIs) and was found to block activation of RhoA in *Yersinia*-infected cells (19–21). Interestingly, the kinase activity of YopO is activated by actin (22). It has remained unclear whether kinase activity contributes to F-actin disruption and antiphagocytic activity of YopO or whether these effects are solely due to inactivation of Rho GTPases. Clearly the kinase activity of YopO is relevant *in vivo* given that yersiniae expressing kinase-deficient YopO mutants are reduced in mouse virulence by at least 2 orders of magnitude (16, 23).

We report here that YopO binds to G-actin via two separate binding sites, which leads to its autophosphorylation. Autophosphorylation up-regulates YopO capability to phosphorylate external substrates. Cellular analysis indicated that YopO

kinase specifically controls cell rounding and inhibits a *Yersinia*-specific internalization mechanism. We propose that these YopO effects are connected to the G-actin-triggered activation process described herein.

## EXPERIMENTAL PROCEDURES

*Materials and Cell Culture*—Chemical reagents were from Sigma-Aldrich, Roche Diagnostics, or Merck if not otherwise indicated. Oligonucleotides were from Metabion (Martinsried, Germany) or MWG (Ebersberg, Germany). The pGEX-6P-2 plasmids encoding GST-YopOwt and GST-YopOK269A were a generous gift of J. Dixon and S. Juris (University of Michigan). Human brain microvascular endothelial cells (HBMEC) and human umbilical vein endothelial cells were grown in ECGM from PromoCell (Heidelberg, Germany), 10% fetal bovine serum in plastic culture flasks at 37 °C, 5% $CO_2$ in a humidified atmosphere. Human monocytes were isolated and cultivated as described (30).

*Purification of Actin*—Skeletal muscle actin was prepared according to Spudich and Watt (24) and further purified on a S200 gel filtration column, and the concentration of actin was measured as described by Wegner (25). For the preparation of actin from *Dictyostelium discoideum*, the soluble extract was chromatographed on a DE52 column ($5 \times 30$ cm) using a linear salt gradient of 0–350 mM NaCl ($2 \times 750$ ml) essentially as described (26). Human platelet G-actin was purchased from tebu-bio (Offenbach, Germany).

*Fluorescence Spectroscopy*—Actin was labeled with *N*-(1-pyrenyl)iodoacetamide (pyrene) according to Kouyama and Mihashi (27). Aliquots of pyrene-labeled actin were frozen in liquid nitrogen and stored at $-70$ °C. Before use, the pyrene-labeled G-actin was thawed quickly and dialyzed in buffer containing 2 mM Tris/HCl, pH 8.0, 0.2 mM ATP, 0.5 mM DTT, 0.2 mM $CaCl_2$ overnight. For the measurement of actin polymerization a mixture of pyrene-labeled and unlabeled G-actin in a molar ratio of 1:10 was used at a final concentration of 2.2 $\mu$M with or without YopO constructs. The measurements were performed at room temperature in a luminescence spectrometer (Aminco Bowman). For kinetic measurements the excitation wavelength was 365 nm, and the emission wavelength was 386 nm.

*Construction of Plasmids and Expression of Proteins*—Plasmid DNA preparations and isolation of DNA fragments from agarose gels were performed with Qiagen kits (Hilden, Germany). Restriction endonuclease digestions and PCR were performed according to standard protocols. The 5′ and 3′ deletions of *yopO* were constructed by PCR with the respective primers denoted in supplemental Table 1 using *Y. enterocolitica* O:8 *yopO* as template (28). Identity to the published YopO sequence on pYV8081 (accession number NP_863565) was verified. PCR products were subcloned using EcoRI and XhoI restriction sites and in-frame fusion with GST into pGEX-4T-1 or -2. The vector for expression of GST-YopO-(700–729) was constructed by inserting an oligonucleotide corresponding to amino acids 700–729 of *yopO* into pGEX-4T-2.

For construction of vectors expressing GFP-YopO fusion proteins, the corresponding *yopO* fragments were introduced into the mammalian expression vector pEGFP-C1 (BD Clontech Laboratories). YopO amino acid substitutions were intro-

duced using QuikChange®II site-directed mutagenesis kit (Stratagene, Amsterdam, The Netherlands) following the manufacturer's instructions, giving rise to the YopOD267A/K269A mutant and the point mutants S95A, S102A, T89A/S95A, S90A/S95A, T89A/S102A, S90A/S102A, D267A/K269A/S90A/S95A.

Plasmids were transformed into *Escherichia coli* BL-21 using a heat shock procedure. For protein expression, overnight bacterial cultures were diluted 1:20 in Luria Bertani medium containing 100 $\mu$g/ml ampicillin and grown at 37 °C to an $A_{600}$ of 0.6–0.8. Bacterial suspensions were shifted to 18 °C, and protein expression was induced for 3–4 h with 0.4 mM isopropyl 1-thio-$\beta$-D-galactopyranoside. After French press, GST proteins were purified from bacterial lysates on glutathione-Sepharose beads 4B (Amersham Biosciences) in lysis buffer containing 50 mM Tris, pH 7.4, 100 mM NaCl, 10% glycerol. Triton X-100 (0.1%) was added for purification of GST-YopOwt and GST-YopOK269A. GST-fused proteins on beads were either eluted with reduced glutathione (30 mM, pH 8.0, in lysis buffer) or cleaved overnight at 4 °C with 50 units of thrombin/ml of settled beads.

*SDS/PAGE, Densitometry, and Western Blot Analysis*—Proteins were separated by 10% SDS/PAGE followed by Coomassie Blue staining. For determination of the YopO-actin binding stoichiometry, the corresponding protein bands from gel filtration fractions containing the actin-YopO complex were quantified by two dimensional densitometry using a Gel Doc EQ System and Quantity One software (Bio-Rad). For Western blot, proteins were transferred by semidry blotting onto polyvinylidene fluoride (PVDF) membranes for 1 h at 1.2 mA/cm². The PVDF membrane was blocked for 1 h or overnight at room temperature or 4 °C, respectively, in phosphate-buffered saline, pH 7.4, 3% bovine serum albumin, 0.05% Tween 20. Membranes were developed with one of the following primary antibodies: anti-YpkA/YopO rabbit polyclonal (1:100,000; 20), anti-phosphoserine/threonine ATM/ATR rabbit polyclonal (1:500; Cell Signaling, New England Biolabs, Frankfurt, Germany). Secondary antibodies were goat anti-mouse or anti-rabbit IgG coupled to horseradish peroxidase (1:2,000 to 1:10,000; Amersham Biosciences). Detection was performed with an enhanced chemiluminescence kit (ECL; Amersham Biosciences).

*Phosphorylation Assays*—Kinase reactions were performed with 3–10 $\mu$g of GST-YopO, YopOwt, or the indicated fragments in 20 $\mu$l of kinase buffer containing 20 mM Hepes pH 7.4, 1.0 mM ATP, 1 mM DTT, 10 mM $MgCl_2$, 2 mM $MnCl_2$ supplemented with 5 $\mu$Ci of [$\gamma$-$^{32}$P]adenosine 5′-triphosphate (Amersham Biosciences) and incubated with 3–10 $\mu$g of *D. discoideum* G-actin for 30 min at 30 °C. Where indicated, human platelet G-actin, *D. discoideum* G-actin, or rabbit skeletal muscle G- or F-actin were added. The reaction was terminated by the addition of $4 \times$ SDS/PAGE sample buffer and heating for 5 min at 95 °C. Radioactivity in dried SDS/PAGE gels or on blot membranes was visualized using phosphorimaging (Fujifilm FLA 3000) and Aida 4.0 Image Analyzer software or by exposure to x-ray film.

*Mass Spectrometry Analysis of Phosphorylated YopO*—YopOwt or mutant proteins were subjected to a phosphorylation reaction (see above) in the presence of 1 mM cold ATP, separated by 10% SDS/PAGE, and stained with Coomassie Blue. Protein

bands were excised and in-gel-digested using modified trypsin (Promega, Mannheim, Germany) according to standard procedures (29). Peptides were desalted using ZipTips (Millipore, Schwalbach, Germany) and either eluted using a saturated α-cyano-4-hydroxycinnamic acid solution in 50% acetonitrile, 0.3% trifluoroacetic acid for matrix-assisted laser desorption ionization time-of-flight analysis or by spray negative ion mode spray solution (50% methanol, 5% ammonium hydroxide) for MS/MS analysis (MS/MS is tandem mass spectrometry (MS)) and precursor ion scans. Precursor ion scans were recorded in negative mode on a Q-STAR XL tandem mass spectrometer detecting all precursor ions that resulted in a product ion with a $m/z$ value of 79 atomic mass units ($PO_3^-$). The charge state of the precursor ions was resolved in a negative ion mode time-of-flight spectrum of the same sample.

*Chromatography and Purification of YopO-Actin Complex*—For preparation of monomeric YopO-(89–729), 500 μg of protein in 50 μl of buffer containing 50 mM Tris/HCl, pH 8.0, 150 mM NaCl, 1 mM DTT, 5 mM MgCl$_2$, 2.5 mM CaCl$_2$ were loaded onto a Superdex 200 PC 3.2/30 column equilibrated with 30 mM Tris/HCl, pH 7.5, 150 mM NaCl, 1 mM DTT in a Smart system (Amersham Biosciences). The flow rate was 40 μl/min, and the fraction size was 50 μl. Fractions eluting shortly before the 66-kDa marker contained monomeric YopO and were combined. Freshly dialyzed *D. discoideum* actin (50 μl, 1 μg/μl) in 2 mM Tris/HCl, pH 8.0, 0.2 mM ATP, 0.5 mM DTT, 0.2 mM CaCl$_2$ was centrifuged for 30 min at 4 °C and 100,000 × g to remove residual F-actin. For preparation of the YopO-actin complex, monomeric YopO-(89–729) and G-actin (1 μg/μl, each) were mixed in gel filtration buffer, incubated for 15 min at room temperature, and then loaded onto the gel filtration column at a flow rate of 40 μl/min and a fraction size of 25 μl. Fractions were analyzed by SDS/PAGE, Coomassie Blue staining or by Western blot analysis as indicated. For dephosphorylation, purified YopO-(89–729)-actin complex was incubated with or without protein serine/threonine phosphatase 1 (2500 units/ml; New England Biolabs) at 30 °C for 1 h and then refractionated on gel filtration columns. Molecular mass markers were sweet potato β-amylase (200 kDa), bovine serum albumin (66 kDa), and bovine erythrocyte carbonic anhydrase (29 kDa).

*GST Pulldown Assays*—*D. discoideum* G-actin (~30 μg in 200 μl of 2 mM Tris/HCl, pH 8.0, 0.2 mM Na-ATP, 0.5 mM DTT, 0.2 mM CaCl$_2$, 0.01% NaN$_3$) was incubated with 50 μl of glutathione-Sepharose beads and loaded with 30 μg of the appropriate GST fusion protein at 4 °C for 1.5 h. Beads were washed 4× with lysis buffer containing 1% Triton-X100 and then subjected to SDS/PAGE and Western blot analysis.

*Analytical Ultracentrifugation*—Sedimentation equilibrium experiments were performed with an analytical ultracentrifuge (Optima XL-I; Beckman Instruments) equipped with absorbance and interference optics. Aluminum double sector cells with sapphire windows were used throughout. Protein solutions containing 0.3 mg of YopO-actin complex per ml were dialyzed against 30 mM Tris/HCl, pH 7.5, 150 mM NaCl. The partial specific volume was estimated from the amino acid composition of YopO and actin yielding a value of 0.737 ml/g. The protein solution was centrifuged at 8064 × g and 4 °C for 72 h.
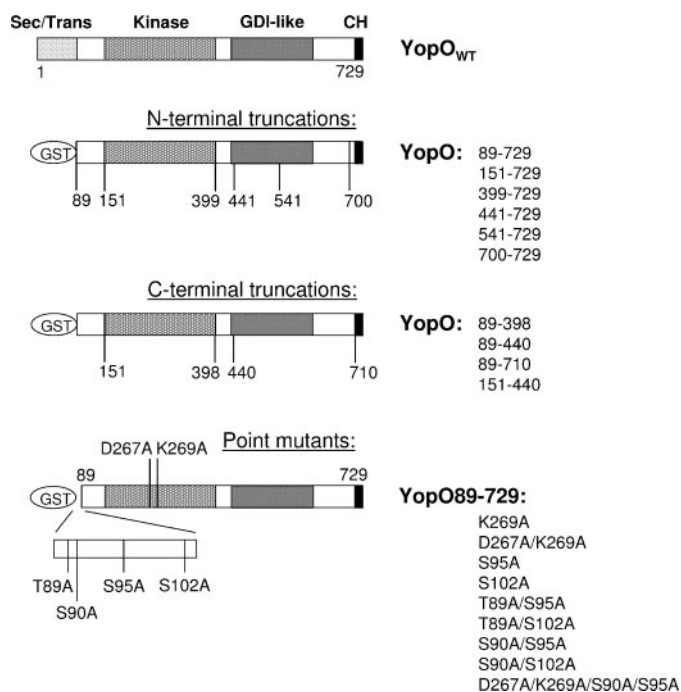
*Cell Rounding, Actin Disruption, and Phagocytosis Assays*—Cells (HBMEC, human umbilical vein endothelial cells, human monocytes) were transiently transfected with vectors expressing GFP or GFP-YopO constructs using Metafectene (Biontex, Martinsried, Germany) or Amaxa nucleofector technology (Amaxa, Cologne, Germany). Cells showing GFP fluorescence were scored for rounding/arborization using phase contrast microscopy and for actin filament disruption using Alexa Fluor 568 phalloidin staining. Only cells with completely rounded phenotype or complete disruption of actin filaments were scored as positive. IgG- or complement coated sheep red blood cells were added at a ratio of 15:1 to human monocytes (30) transfected with vectors expressing GFP or GFP-YopOwt. Intra- and extracellular sheep red blood cells were distinguished by phase contrast microscopy as described (31). *Yersinia* invasin-coated fluorescent latex beads were attached to HBMEC (50:1) expressing GFP, GFP-YopOwt, or GFP-N17Rac. The percentage of internalized beads was determined as described (30). *Yersinia* YadA expressing *E. coli* were attached to cells expressing the indicated GFP-YopO constructs (ratio 30:1), and internalized bacteria were quantified with a double immunofluorescence staining method as described (30, 32). Internalization was normalized to control cells that were set to 100%. Statistical evaluation was performed using Student's *t* test. To verify equal expression of GFP fusion proteins, the respective transfected cells were recorded with a spot Pursuit 1.4MP monochrome camera and Spot software (Diagnostic Instruments, Inc, Sterling Heights, MI) using identical exposure settings. Average pixel intensities of three outlined regions per cell were obtained using ImageJ software (Research Services Branch, National Institute of Mental Health) and imported into graphics program for statistical analysis.

## RESULTS

*YopO Autophosphorylation Is Stimulated by G-actin*—The modular protein organization of YopO is depicted in Fig. 1. The N-terminal region mediating bacterial secretion/translocation and membrane localization in host cells is followed by the predicted kinase domain (amino acids 150–400). The C-terminal half of YopO contains a Rho GTPase binding GDI-like domain (within amino acids 431–612) and a stretch of amino acids (amino acids 710–729) displaying homology to the actin bundling protein coronin. This domain model is a synopsis of all published structural and biochemical data of YopO and YpkA (9, 16, 19, 21, 22, 33).

To determine which form of actin stimulates YopO kinase, we assayed autophosphorylation of recombinant wild type YopO (YopOwt) in the presence of G-actin or F-actin. As described before (22), no autophosphorylation of YopO occurred in the absence of actin. By comparison, YopO autophosphorylation was detectable already at a G-actin:YopO molar ratio of 0.1:1 and was maximal at a 1:1 ratio. In contrast, even a 5-fold molar excess of F-actin *versus* YopO did not significantly stimulate YopO autophosphorylation (Fig. 2a).

We also investigated whether muscle and nonmuscle actins differ in their ability to stimulate YopO. These experiments showed that human platelet actin and *D. discoideum* actin were
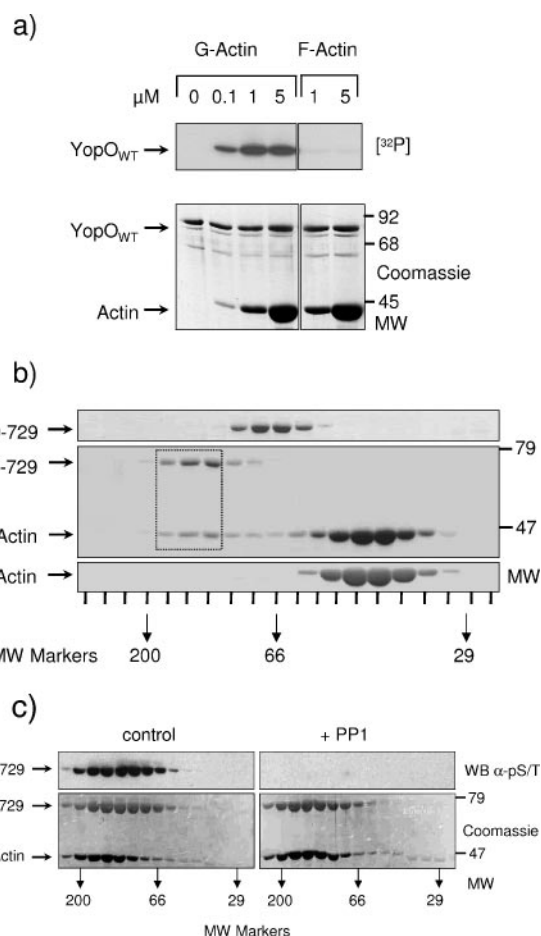
FIGURE 1. **Scheme of YopO protein organization and YopO constructs used in this study.** The first and the last amino acids of YopOwt or its fragments and mutants are indicated. cDNAs encoding these constructs were cloned into vectors, allowing expression of GST fusion proteins in *E. coli* or GFP fusion proteins in host cells. *Sec/Trans*, secretion and translocation region used by the *Yersinia* type III secretion system. *Kinase*, region with homology to serine/threonine kinases. Asp-267 and Lys-269 are amino acids critical for catalytic activity. *GDI-like*, region with homology to Rho GDI. *CH*, coronin homology region (16, 19, 21, 22).

equally effective in activating YopO autophosphorylation, whereas muscle actin was about a ¹⁄₁₀ as active (supplemental Fig. 1S). Yet at high enough concentrations muscle G-actin could also cause full activation of YopO.[4] Hence, YopO kinase is best activated by nonmuscle G-actin, which fits with the idea that it mainly acts in immune cells such as neutrophils and macrophages (9, 10).
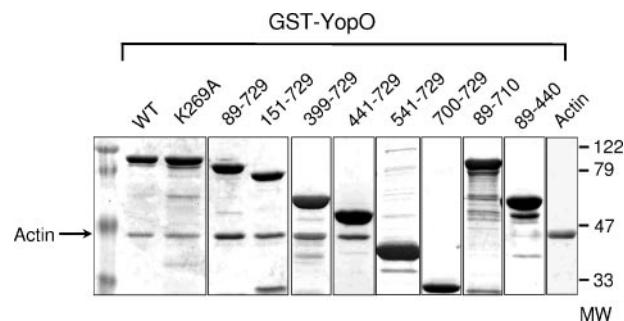
*YopO and Actin Form a Phosphorylation-independent 1:1 Complex*—To get first insights into the mechanism of YopO activation by G-actin, we sought to determine the stoichiometry and molecular mass of the YopO-G-actin complex. Because YopOwt tends to degrade and requires detergents such as Triton X-100 for purification and stability (22), we produced a construct that lacks the N-terminal amino acids 1–88 that serve as the bacterial secretion and translocation signal, giving rise to YopO-(89–729) (Fig. 1). As anticipated, YopO-(89–729) retained all the *in vitro* activities of YopOwt (see below).

To isolate an YopO-actin complex, prepurified monomeric YopO-(89–729) was incubated with *D. discoideum* G-actin. Formation of a complex was verified by gel filtration chromatography. As shown in Fig. 2b, *upper* and *lower panel*, YopO-(89–729) and G-actin individually eluted as monomeric proteins around the 66 kDa and between the 66- and 29-kDa markers, respectively. Upon coincubation, YopO-(89–729) and actin could be detected in fractions eluting between the

---

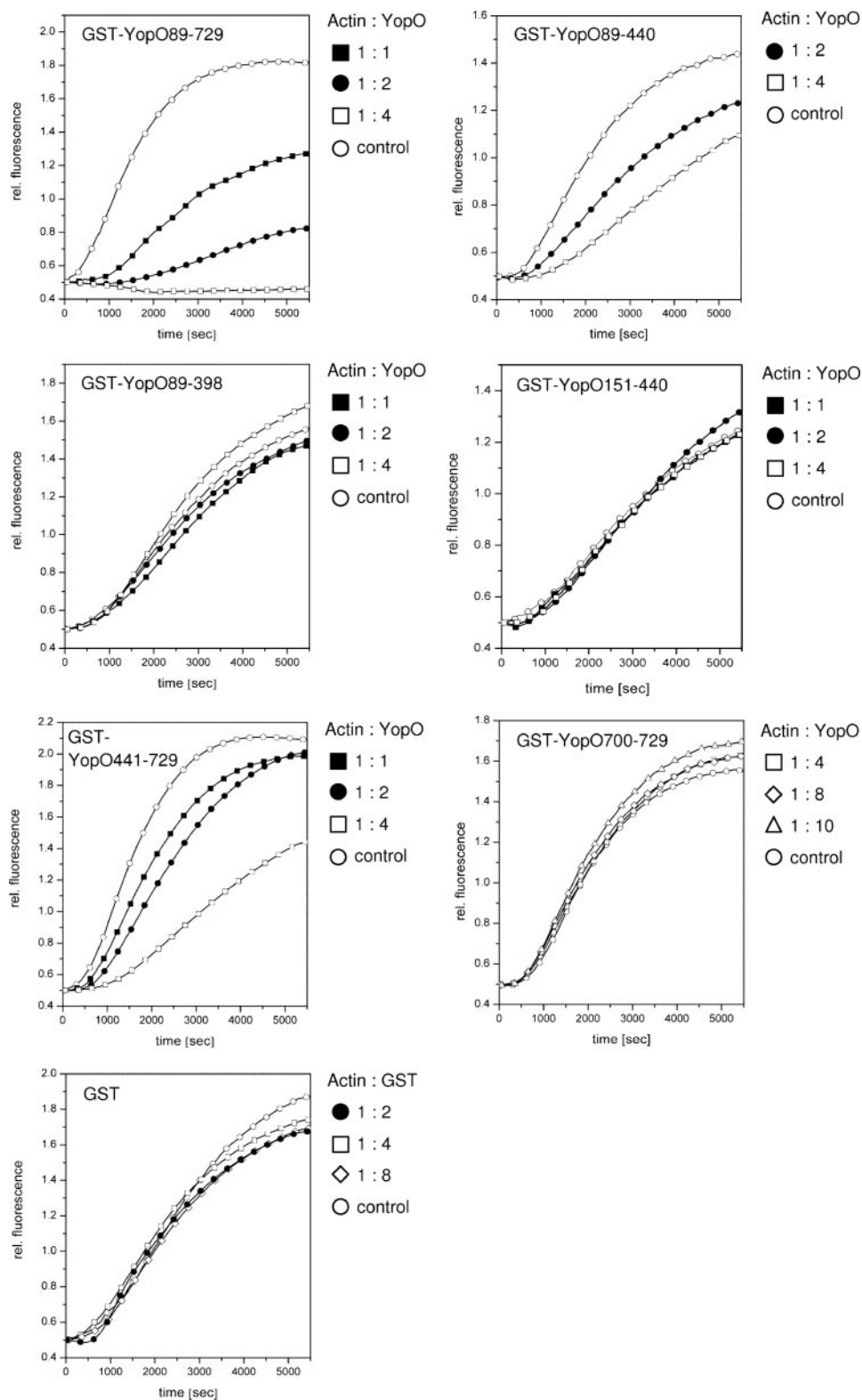[4] G. Yüksekdag, R. Rost, M. Schleicher, and M. Aepfelbacher, unpublished results.

FIGURE 2. **Stimulation of YopO kinase in a 1:1 complex with G-actin.** *a*, YopOwt (1 μM) was incubated with [γ-³²P]ATP and the indicated concentrations of rabbit skeletal muscle G-actin or F-actin. Proteins were separated by 10% SDS/PAGE and visualized by Coomassie Blue staining (*lower panel*). Dried gels were exposed to x-ray film (*upper panel*). Incorporation of radioactivity into YopO was observed in the presence of G-actin but not F-actin. *b*, samples containing monomeric Yop-(89–729) (*upper panel*) or *D. discoideum* G-actin (*lower panel*) or a mixture of both proteins (*middle panel*) were fractionated by gel filtration chromatography and run on SDS/PAGE. *Arrows* indicate elution of molecular weight (*MW*) markers. The YopO-actin complex eluted just after the fractions containing the 200-kDa marker (indicated by the *box*). *c*, fractions containing YopO-actin complex were not treated (control) or were treated with the protein serine/threonine phosphatase PP1 (+*PP1*) and then refractionated by gel filtration chromatography. Dephosphorylation of YopO upon PP1 treatment is verified by anti-phosphoserine/threonine Western blot (*WB, upper panels*). The YopO-actin complex remains intact after YopO dephosphorylation (*lower panels*). The molecular masses of standard marker proteins are indicated in kDa.



FIGURE 3. **GST pulldown identifies the C-terminal G-actin binding region in YopO.** GST pulldown assays were performed with indicated GST-YopO constructs and purified *D. discoideum* G-actin as described under "Experimental Procedures." Proteins were run on SDS/PAGE, blotted onto PVDF membranes, and Coomassie Blue-stained. The molecular masses (*MW*) of standard marker proteins are indicated in kDa.

FIGURE 4. **Actin polymerization assays reveal the N-terminal G-actin binding region in YopO.** Polymerization of 2.2 $\mu$M G-actin was monitored by the increase of fluorescence emission (*rel. fluorescence*) of pyrene-labeled actin in the absence or presence of indicated GST-YopO constructs and plotted *versus* time. The molar ratio of G-actin to GST-YopO constructs was 1:1 (■), 1:2 (●), 1:4 (□), 1:8 (◇), or 1:10 (△). The control contained buffer only (○).
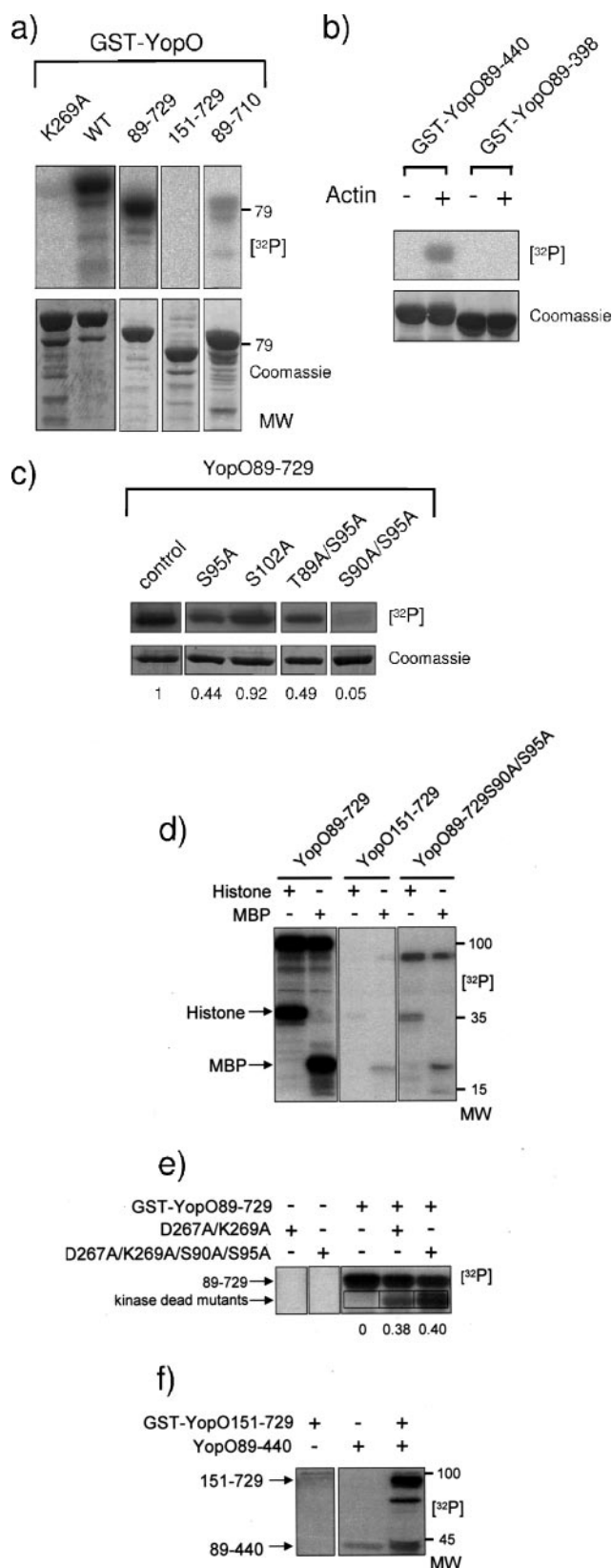
complex by densitometry of Coomassie Blue-stained gels using separate dilution series for calibration. The molar ratio of YopO to actin was determined as 1:1.

To directly measure the mass of the YopO-actin complex, sedimentation equilibrium ultracentrifugation was performed (see supplemental Fig. 2*S* for a representative experiment). These experiments yielded a molecular mass of 126 ± 6 kDa (mean ± S.D.; $n = 2$) for the YopO-actin complex purified by gel filtration chromatography (fractions corresponding to the *boxed lanes* in Fig. 2*b* were used). This clearly indicated that the YopO-actin complex consists of one molecule of actin and one molecule of YopO.

We also tested whether dephosphorylation of YopO has an effect on the stability of the YopO-actin complex. By using an anti-phosphoserine/threonine antibody (see supplemental Fig. 3S) it was first verified that YopO in the complex with actin was phosphorylated (Fig. 2*c*). The purified complex was treated with the nonspecific protein serine/threonine phosphatase 1 and again loaded onto the gel filtration column. As documented in Fig. 2*c*, the complex of dephosphorylated YopO and actin remained stable. We, therefore, conclude that YopO is phosphorylated upon forming a 1:1 complex with G-actin, but phosphorylation is not required for the stability of the complex.

*YopO Contains Separate N- and C-terminal G-actin Binding Sites*— To delineate the regions of YopO involved in actin binding, we performed pulldown assays using purified *D. discoideum* G-actin and N- and C-terminal deletion mutants of YopO fused to GST (depicted in Fig. 1). As demonstrated in Fig. 3, GST-YopO-(89–729) and kinase-defective GST-YopOK269A bound as effectively to actin as GST-YopOwt, indicating that neither the N-terminal secretion/translocation region nor autophosphorylation of YopO is necessary for actin binding. GST-YopO-(151–729), GST-YopO-(399–729), and GST-YopO-(441–729) all pulled down G-actin. In contrast, GST-YopO-(541–729) and GST-YopO-

200- and 66-kDa markers, indicating formation of an YopO-actin complex (Fig. 2*b*, *middle panel*). To determine the YopO-actin stoichiometry, we quantified the two proteins within the

FIGURE 5. **Characterization of YopO kinase reactions.** *a*, autophosphorylation of wild type and mutant YopO proteins. Indicated GST-YopO constructs were incubated with [$\gamma$-$^{32}$P]ATP and *D. discoideum* G-actin, run on SDS/PAGE, and blotted onto PVDF membrane. *Upper panel*, autoradiography; *lower panel*, Coomassie Blue staining. *b*, autophosphorylation of YopO kinase region 89–440 upon stimulation with G-actin. GST-YopO-(89–440) or GST-YopO-(89–398) were incubated with [$\gamma$-$^{32}$P]ATP and, with or without

(700–729), containing the putative C-terminal actin binding domain and the coronin homology region, respectively, did not pull down actin (21, 22). As reported before, YopO-(89–710) was unable to bind to actin in this assay (22; Fig. 3). Consequently, YopO-(89–440) harboring the predicted catalytic domain and lacking the C-terminal half of the protein did not present actin binding activity either (Fig. 3). These results indicate that the C-terminal portion of YopO harbors an actin binding site for which amino acids 441–729 are necessary and sufficient. In experiments aimed to narrow down the YopO catalytic domain, we noticed that YopO-(89–440) harboring the kinase region displayed autophosphorylation in the presence but not in the absence of G-actin (data in Fig. 5*b*). This indicated that the N-terminal half of YopO-(89–440) must also have the capability to associate with actin even though this could not be detected by GST pulldown assays. We, thus, employed an alternative method to determine G-actin binding of YopO-(89–440). Proteins that sequester G-actin can inhibit polymerization of G-actin to F-actin *in vitro*, thus allowing the calculation of bound *versus* free G-actin and an approximate $K_d$ of the G-actin-sequestering protein complex. In this assay YopO-(89–729) dose-dependently inhibited actin polymerization; the $K_d$ of the YopO-(89–729)-G-actin complex was estimated to be ~1.9 $\mu$M. Under these conditions similar values have been determined for the G-actin-sequestering profilins I (5.1 $\mu$M) or II (1.8 $\mu$M) from *D. discoideum* (34). As inferred from its actin-dependent autophosphorylation activity, YopO-(89–440) also inhibited formation of F-actin in the assay. A rough calculation yielded a $K_d$ of 4.1 $\mu$M for the YopO-(89–440)-G-actin complex. In contrast, YopO-(89–398) and YopO151–440 showed no inhibitory activity in this assay (Fig. 4). Additional actin polymerization assays indicated that YopO-(441–729) ($K_d$ 6.1 $\mu$M) and YopO-(399–729) ($K_d$ 5.5 $\mu$M) also sequester G-actin, which is consistent with the GST pulldown data (Fig. 4 and not shown). We conclude from this data that YopO harbors two independent actin binding sites. One is encompassed by amino acids 89–440, whereby amino acids 399–440 are essential. The other is formed by amino acids 441–729, whereby amino acids 710–729 are essential. Because of the 1:1 stoichiometry of the YopO-G-actin complex, we also conclude that the N- and C-terminal portions of YopO bind to different regions of the actin molecule.

*D. discoideum* G-actin, run on SDS/PAGE and blotted onto PVDF membranes. *Upper panel*, autoradiography; *Lower panel*, Coomassie Blue staining. *c*, activity of YopO phosphorylation site mutants. YopO-(89–729) constructs harboring indicated single or double point mutations were subjected to kinase reaction and run on SDS/PAGE. *Upper panels*, autoradiography. *Lower panels*, Coomassie Blue staining. The *numbers* indicate relative intensities of $^{32}$P radiation whereby the value of YopO-(89–729) (control) was arbitrarily set to 1. *d*, autophosphorylation of YopO controls substrate phosphorylation. Indicated YopO constructs were subjected to kinase reaction in the presence of designated artificial substrates, run on SDS/PAGE, and subjected to autoradiography. *MBP*, myelin basic protein. *e*, transphosphorylation of kinase dead YopO mutants by YopO. GST-YopO-(89–729) and designated point mutants of YopO-(89–729) were subjected to kinase reaction followed by SDS/PAGE and autoradiography. The *numbers* indicate intensities of $^{32}$P radiation relative to the values of YopO-(89–729) atop that were arbitrarily set to 1. *f*, transphosphorylation of YopO-(151–729) by YopO-(89–440). YopO-(89–440) was coincubated with GST-YopO-(151–729) and subjected to kinase reaction followed by SDS/PAGE and autoradiography. The molecular masses (*MW*) of standard marker proteins are indicated in kDa.

**TABLE 1**

**Summary of the mass spectrometry results**

Indicated constructs were *in vitro* phosphorylated, digested with trypsin, and then investigated with precursor ion scanning. The left column shows the number of experiments performed, and the right column shows the number of phosphate groups found in the designated YopO peptides.

| No. of experiments | Construct | $m/z$ [M-zH]z- | Corresponding peptide[a] | YopO sequence | No. of phosphates |
|---|---|---|---|---|---|
| 3 | YopO-(89–729) | 944, 944, 945 [M-3H]3- | GSPEFTSQELRSDIPNALSNLFGAK | 89–108 | 2 |
| 3 | YopO-(89–729) | 663, 663, 663 [M-2H]2- | GSPEFTSQELR | 89–94 | 1 |
| 3 | YopO-(89–729) | 760, 761, 762 [M-2H]2- | SDIPNALSNLFGAK | 95–108 | 1 |
| 3 | YopO-(89–729)S102A | 939, 939, 939 [M-3H]3- | GSPEFTSQELRSDIPNALANLFGAK | 89–108 | 2 |
| 2 | YopO-(89–729)S90A/S102A | 907, 907 [M-3H]3- | GSPEFTAQELRSDIPNALANLFGAK | 89–108 | 1 |
| 2 | YopO-(89–729)S90A/S102A | 754, 753 [M-2H]2- | SDIPNALANLFGAK | 95–108 | 1 |

[a] GSPEF was derived from pGEX vector.

*N- and C-terminal Actin Binding Is Required for Full Activity of YopO*—To characterize the interplay of kinase activation and actin binding, we tested autophosphorylation of YopO deletion mutants upon stimulation with actin. As demonstrated in Fig. 5a, YopOwt and YopO-(89–729) showed comparable incorporation of radioactivity, consistent with their intact N- and C-terminal actin binding sites. YopO-(151–729) was kinase-dead, which may be due to disruption of its N-terminal actin binding site but could also be caused by removal of autophosphorylation sites (see below). YopOK269A displayed low residual autophosphorylation. Interestingly, YopO-(89–440), which consists of the N-terminal kinase region and actin binding site, was capable of autophosphorylating in the presence but not in the absence of actin (Fig. 5b). In comparison, YopO-(89–398) showed no autophosphorylation (Fig. 5b), consistent with its abolished actin binding (Fig. 4). Autophosphorylation of YopO-(89–440) was considerably diminished compared with YopO-(89–729) and closely resembled that of YopO-(89–710) (compare Fig. 5, a and b). Because YopO-(89–710) essentially lacks the amino acids required for C-terminal actin binding (Fig. 3), these data strongly indicate that YopO requires simultaneous binding of G-actin to its N- and C-terminal regions for full stimulation of kinase activity.
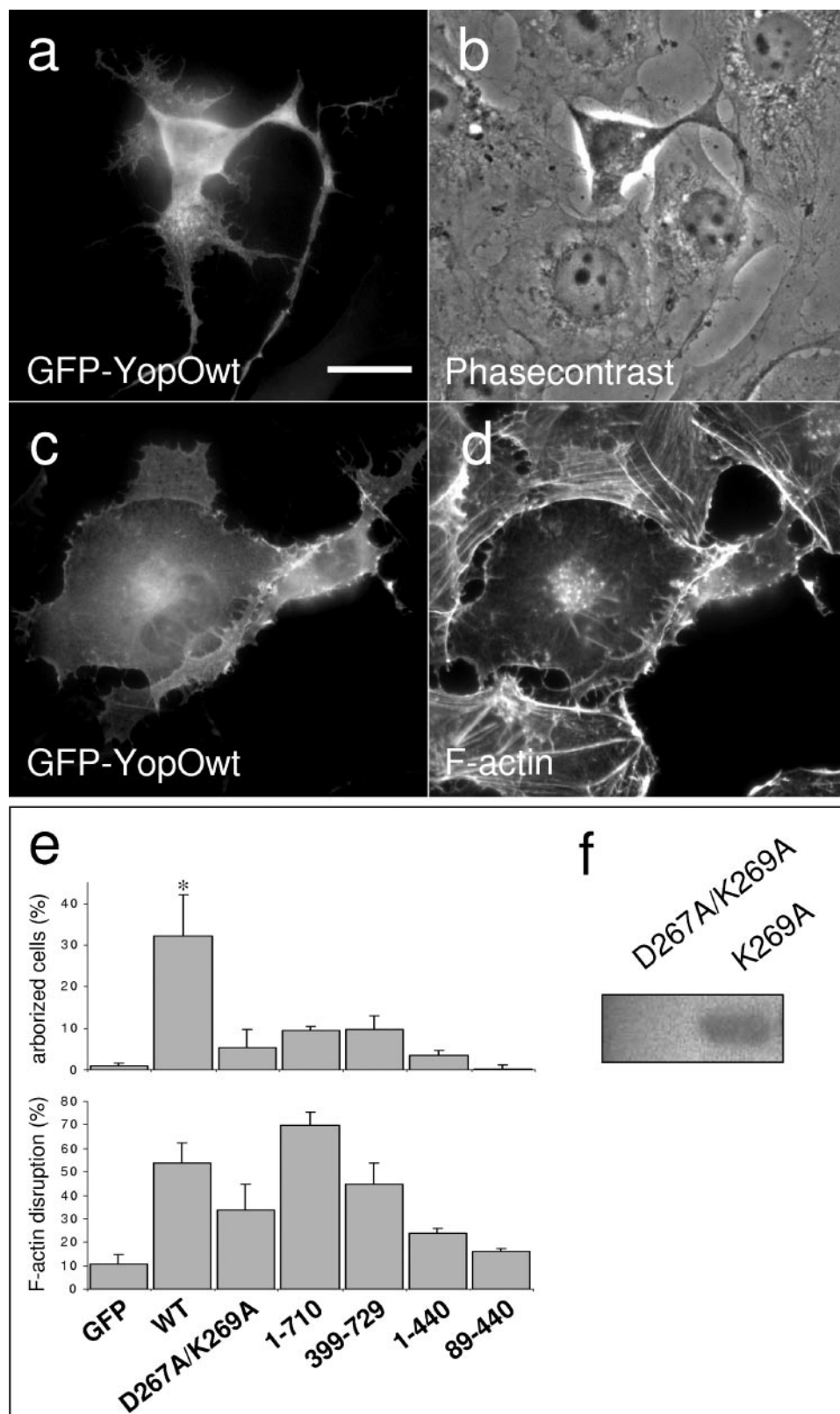
*Identification of Autophosphorylated Amino Acids in YopO That Regulate Its Kinase Activity*—For identification of autophosphorylated amino acid residues in YopO, we performed MS analysis of *in vitro* phosphorylated YopO-(89–729). By employing precursor ion scanning, a peptide corresponding to amino acids 89–108 of YopO (peptide 89–108) containing two phosphate groups was detected. In addition, peptides 89–94 and 95–108, each containing one phosphate group, were found (summarized in Table 1). This indicates that there are two phosphorylated residues within amino acids 89–108 of YopO whereby one lies within peptide 89–94 (Thr-89 or Ser-90) and the other one within peptide 95–108 (Ser-95 or Ser-102). To identify the relevant site within amino acids 95–108, we analyzed the single point mutants YopOS95A and YopOS102A. Two phosphorylated residues could be detected within peptide 89–108 of YopOS102A, implicating Ser-95 as a phosphorylation site. No signals were detected with YopOS95A. We next analyzed the following double point mutants of YopO-(89–108): T89A/S95A, T89A/S102A, S90A/S95A, and S90A/S102A. The results obtained with YopOS90A/S102A were revealing given that peptides 89–108 and 95–108 were detected and that each contained one single phosphorylated residue (Table 1). This result not only confirmed Ser-95 as a phosphorylation site (by exclusion of Ser-102) but also sug-

gested that Ser-90 is the second site; otherwise, a doubly phosphorylated peptide 89–108 should have been detected. No conclusive results could be obtained with the other double point mutants. The reason might be that some of these mutations reduce autophosphorylation/incorporation of radioactivity into YopO and/or alter the chemical properties of the generated peptides.

To verify the phosphorylation sites putatively identified by MS, we subjected the following single or double point mutants of Yop-(89–729) to kinase assays: S95A, S102A, S90A/S95A, and T89A/S95A. Consistent with the MS data, incorporation of radioactivity was unchanged in YopOS102A and reduced by about 50% in YopOS95A and YopOT89A/S95A. Importantly, autophosphorylation was greatly diminished by about 90% in YopOS90A/S95A (Fig. 5c). These data clearly establish that amino acid residues Ser-90 and Ser-95 are autophosphorylation sites within YopO.

Next we asked whether autophosphorylation of YopO on Ser-90/Ser-95 also regulates phosphorylation of external substrates. The data presented in Fig. 5d reveal that YopO-(89–729)S90A/S95A displayed greatly diminished phosphorylation of the artificial substrates myelin basic protein and histone. This indicates that autophosphorylation of YopO on Ser-90/Ser-95 activates its kinase activity. In line with this, YopO-(151–729) lacking the autophosphorylation sites did not present any substrate phosphorylation.

To get an idea whether autophosphorylation occurs by an intermolecular or rather an intramolecular process, we checked for (trans)phosphorylation of the kinase dead YopOD267A/K269A and YopOD267A/K269A/S90A/S95A by YopO-(89–729). YopOD267A/K269A and YopO D267A/K269A/S90A/S95A were both substrates of YopO-(89–729). Both mutants incorporated the same amount of radioactivity, suggesting that Ser-90 and Ser-95 are not preferably phosphorylated by an intermolecular process and more likely by an intramolecular process (Fig. 5e). These data together with the residual autophosphorylation of the YopOS90A/S95A mutant also point to an additional (trans)phosphorylation site in YopO besides Ser-90 and Ser-95. This must be another serine residue because phosphorylated YpkA only contains phosphoserines (16). The capability of YopO-(89–440) to transphosphorylate YopO-(151–729) supports this notion (Fig. 5f). That YopO-(89–710) could not be transphosphorylated also indicates the requirement of C-terminal actin binding for transphosphorylation (supplemental Fig. 4S). By mass spectrometry a putatively transphosphorylated amino acid was detected in YopO-(151–729), but despite production of a corresponding point mutant, YopO-
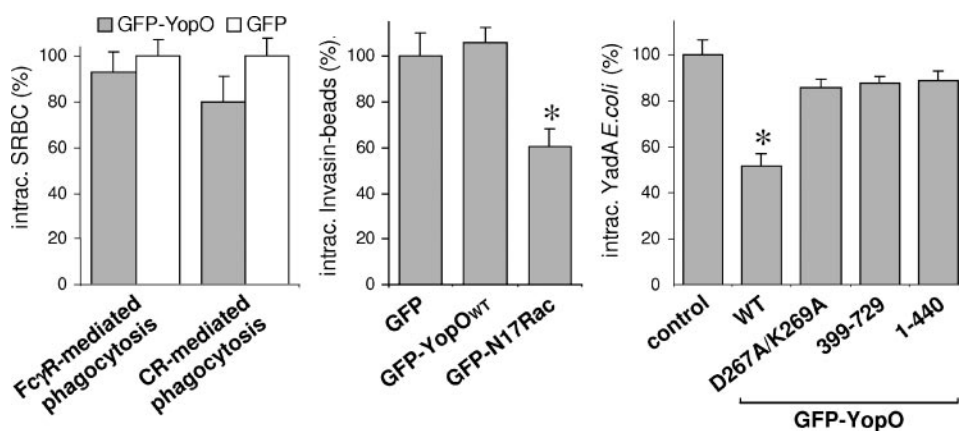
FIGURE 6. **Effect of YopO and YopO mutants on cell rounding/arborization and disruption of stress fibers.** *a* and *c*, HBMEC expressing GFP-YopOwt were evaluated by phase contrast microscopy to reveal cell arborization (*b*) or Alexa Fluor 568 phalloidin staining to check for F-actin disruption (*d*). *e*, quantification of cell arborization and F-actin disruption induced by GFP-YopOwt or the indicated GFP-YopO constructs. Values are the mean ± S.D. of three experiments. For each experiment ≥90 cells per condition were evaluated. An *asterisk* indicates significant different values between YopOwt and YopOD267A/K269A ($p < 0.01$). *f*, kinase activity of YopOK269A and YopOD267A/K269A. Equal amounts of protein were subjected to kinase reaction, run on SDS/PAGE, and monitored by autoradiography.

(151–729) still could be transphosphorylated. One interpretation is that if one phosphorylation site is removed, it may be substituted by other normally not phosphorylated sites. In summary, YopO kinase is activated by actin-triggered autophosphorylation on Ser-90 and Ser-95.

*Kinase Activity Determines Specific Cellular Effects of YopO*—Because here we have separated the different YopO activities and characterized the correspondent YopO protein constructs *in vitro*, we could investigate how kinase, actin, and Rho binding functions contribute to the cellular effects of YopO. Transfection of HBMEC with a vector expressing GFP-YopOwt induced cell rounding associated with arborization (32 ± 10%) and disruption of actin stress fibers (54 ± 9%; Fig. 6). Because YopOK269A still has residual kinase activity, we constructed YopOD267A/K269A in which a second critical residue in the catalytic loop of YopO is mutated (19, 22). YopOD267A/K269A showed no detectable autophosphorylation (Fig. 6*f*), and it produced significantly less cell arborization than GFP-YopOwt (Fig. 6*e*). Consistent with this, YopO-(1–710), YopO-(1–440), and YopO-(89–440), which display greatly reduced kinase activity, as well as YopO-(399–729), lacking the N-terminal kinase region altogether, also induced much less cell arborization than YopOwt (Fig. 6*e*). This suggests that the kinase activity of YopO determines cell rounding. Furthermore, because YopOwt, YopOD267A/K269A, YopO-(1–710), and YopO-(399–729) all disrupted actin filaments and YopO-(1–440) and YopO-(89–440) were essentially without effect, we conclude that actin filament disruption is caused by the C-terminal GDI-like domains of YopO. Finally, because the cellular effects and the actin binding capabilities of the different YopO constructs do not correlate (Figs. 3, 4, and 6), YopO does most likely not act by just sequestering actin.

FIGURE 7. **YopO effect on different phagocytosis mechanisms.** *Left*, IgG- or complement-coated sheep red blood cells were added at a ratio of 15:1 to human macrophages expressing GFP or GFP-YopOwt. Percentage of internalized sheep red blood cells was quantified using phase contrast microscopy (31). *Middle*, *Yersinia* invasin-coated fluorescent latex beads were attached to HBMEC (ratio 50:1) expressing GFP, GFP-YopOwt, or GFP-N17Rac. Percentage of internalized beads was quantified as described (30). *Right*, *Yersinia* YadA-expressing *E. coli* were attached to human umbilical vein endothelial cells (ratio 30:1) expressing the indicated GFP-YopO constructs. The percentage of internalized bacteria was determined by an immunofluorescence method as described (30). All values are the mean ± S.D. of three experiments with ≥90 cells evaluated per condition and experiment. Internalization was normalized to control cells that were set to 100%. An *asterisk* indicates significant difference to control or GFP.

Although there is indirect evidence for contribution of YopO to the antiphagocytic activity of yersiniae, an effect of YopO on a defined phagocytosis mechanism has not been described (18, 23). Yersiniae employ the Yops that they transfer into target cells to block their uptake by phagocytes (9–12). Opsonized yersiniae are taken up by professional phagocytes via Fcγ receptors or complement receptors. Internalization of non opsonized yersiniae is mediated by the adhesins invasin or YadA and integrin receptors of host cells (9–12, 18). To test whether YopO affects Fcγ receptor- or complement receptor-mediated phagocytosis, we evaluated uptake of IgG- or complement-coated sheep red blood cells by human macrophages expressing GFP or GFP-YopOwt. No effect of YopO on these two phagocytosis mechanisms was detectable (Fig. 7). Next we tested uptake of *Yersinia* invasin-coated beads and *Yersinia* YadA-expressing *E. coli* by human endothelial cells expressing GFP- or GFP-YopOwt. Invasin-mediated internalization was not affected by YopO but, as shown before, was inhibited by dominant negative Rac1 (30). In contrast, YadA-mediated bacterial uptake was significantly reduced in GFP-YopOwt-expressing cells (Fig. 7). This effect depended on full YopO kinase activity because YopOD267A/K269A as well as YopO-(1–440) and YopO-(399–729) were ineffective in this assay (Fig. 7). We conclude that the kinase activity of YopO determines cell rounding/arborization and specifically inhibits *Yersinia* phagocytosis mediated by the adhesin YadA. In comparison, the C terminus of YopO is responsible for actin filament disruption, but actin binding of YopO does not by itself affect the actin cytoskeleton.

## DISCUSSION

Our data indicate that YopO kinase from pathogenic yersiniae becomes activated upon binding to G-actin but is unresponsive to F-actin. To our knowledge YopO constitutes the first G-actin-activated protein kinase described in eukary-

otic or prokaryotic cells. In comparison, the mammalian Abl tyrosine kinase gets inhibited by F-actin and through this mechanism is thought to sense transition of cells from an adherent state with high F-actin content to a detached state with low F-actin content (8). We identified two independent actin binding sites in the N- and C-terminal half of YopO. In the isolated N-terminal kinase region (YopO-(89–440)) moderate autophosphorylation and phosphorylation of substrates can be stimulated by G-actin binding. However, for full kinase stimulation, concomitant actin binding to the N- and C-terminal sites of YopO is required. Thereby one molecule of actin binds to one molecule of YopO. Amino acids Ser-90 and Ser-95 were identified as autophosphorylation sites in YopO. These amino acids were not preferentially phosphorylated by an intermolecular process and are, therefore, most likely phosphorylated intramolecularly. Autophosphorylation on Ser-90 and Ser-95 was a prerequisite for efficient phosphorylation of substrates, suggesting that it represents an autoactivation mechanism. From these data a possible scenario of YopO activation evolves; by embracing an actin molecule with its N- and C-terminal regions, a YopO molecule autophosphorylates on amino acids Ser-90 and Ser-95. Autophosphorylation further stimulates YopO kinase activity and is essential for phosphorylation of external substrates. These results provide useful information as to the expected molecule dynamics of YopO upon actin binding. Clearly, much more precise structural details will be obtained by crystallization of a YopO-actin complex.

We can only speculate about the purpose of kinase activation by G-actin. Because G-actin is always available in target cells, it may merely serve as a default activator of YopO/YpkA. Yersiniae that do not express actin would be protected from premature YopO activation. A more interesting possibility is that YopO may function as a sensor responding to local changes of G-actin concentration. Consistent with this notion, the calculated $K_d$ of the YopO-actin complex is similar to the $K_d$ of the profilin-actin complex, which is effectively regulated by G-actin concentration (34). It is also noteworthy that the mammalian protein MAL was shown to respond to a decrease in G-actin concentration by translocating into the nucleus and activating transcription of the serum response factor gene. Furthermore, MAL activation is in turn controlled by Rho signaling to actin (6). Yet, attempts to relate Rho binding and actin-stimulated kinase activity in YopO/YpkA have indicated that association with Rho or Rac does not influence YopO/YpkA phosphorylation stimulated by actin, and vice versa, autophosphorylation does not influence Rho or Rac binding (19, 20).

It is well established that by modulating Rho GTPase activities, yersiniae subvert immune cell responses such as chemo-

taxis and phagocytosis (10–12). Also, the function of the *Yersinia* type III secretion system translocation pore itself is controlled by actin and by Yop effectors modulating Rho GTPases (35). Thus, YopO may integrate signals from Rho GTPases and changes in G-actin concentration in *Yersinia*-infected cells.

Here we could also identify cellular effects of YopO that are directly related to its kinase activity. The kinase-dead mutant YopOD267A/K269A produced much less cell rounding/arborization but a similar extent of F-actin disruption as YopOwt, indicating that the kinase activity specifically acts back on the cytoskeleton. The YopO kinase activity was also required for inhibition of YadA-mediated phagocytosis, whereas other routes of phagocytosis were unaffected by YopO. This points to a unique role for YopO kinase in modulating cell shape/motility and a *Yersinia*-specific subtype of phagocytosis.

A major question is which cellular substrates are responsible for the YopO kinase effects. Recently ovarian tumor domain ubiquitin aldehyde binding 1 (otubain-1) was identified as a phosphorylation substrate of YopO (36). Otubain-1 is a putative ubiquitinase and associates with the E3 ubiquitin ligase GRAIL, implicated in regulating anergy in lymphocytes (37). However, the consequences of otubain-1 phosphorylation and its putative role in cytoskeletal regulation are elusive.

Because no bacterial or mammalian kinases activated by G-actin have been characterized so far, YopO represents a prototype. It will be interesting to find out which advantage *Yersinia* takes of exploiting cellular G-actin homeostasis for regulating its activity. Once thought to be merely a structural protein of the cytoskeleton, it has now become evident that actin can directly regulate the function of numerous signaling proteins. Some of these may turn out to act as G-actin regulated kinases like YopO.

## REFERENCES

1. Pollard, T. D., and Borisy, G. G. (2003) *Cell* **112,** 453–465
2. Merrifield, C. J. (2004) *Trends Cell Biol.* **14,** 352–358
3. Gouin, E., Welch, M. D., and Cossart, P. (2005) *Curr. Opin. Microbiol.* **8,** 35–45
4. Winder, S. J., and Ayscough, K. R. (2005) *J. Cell Sci.* **118,** 651–654
5. Visa, N. (2005) *EMBO Rep.* **6,** 218–219
6. Miralles, F., Posern, G., Zaromytidou, A. I., and Treisman, R. (2003) *Cell* **113,** 329–342
7. Philimonenko, V. V., Zhao, J., Iben, S., Dingova, H., Kysela, K., Kahle, M., Zentgraf, H., Hofmann, W. A., de Lanerolle, P., Hozak, P., and Grummt, I. (2004) *Nat. Cell Biol.* **6,** 1165–1172
8. Woodring, P. J., Hunter, T., and Wang, J. Y. (2001) **276,** 27104–27110
9. Cornelis, G. R., Boland, A., Boid, A. P., Geuijen, C., Iriarte, M., Neyt, C., Sory, M. P., and Stainier, I. (1998) *Microbiol. Mol. Biol. Rev.* **62,** 1315–1352
10. Cornelis, G. R., and Wolf-Watz, H. (1997) *Mol. Microbiol.* **23,** 861–867
11. Aepfelbacher, M., and Heesemann, J. (2001) *Int. J. Med. Microbiol.* **291,** 269–276
12. Juris, S. J, Shao, F., and Dixon, J. E. (2002) *Cell Microbiol.* **4,** 201–211
13. von Pawel-Rammingen, U., Telepnev, M. V., Schmidt, G., Aktories, K., Wolf-Watz, H., and Rosqvist, R. (2000) *Mol. Microbiol.* **36,** 737–748
14. Zumbihl, R., Aepfelbacher, M., Andor, A., Jacobi, C. A., Ruckdeschel, K., Rouot, B., and Heesemann, J. (1999) *J. Biol. Chem.* **274,** 29289–29293
15. Shao, F., Merritt, P. M., Bao, Z., Innes, R. W., and Dixon, J. E. (2002) *Cell* **109,** 575–588
16. Galyov, E. E., Hakansson, S., Forsberg, A., and Wolf Watz, H. (1993) *Nature* **361,** 730–732
17. Hakansson, S., Galyov, E. E., Rosqvist, R., and Wolf Watz, H. (1996) *Mol. Microbiol.* **20,** 593–603
18. Grosdent, N., Maridonneau-Parini, I., Sory, M. P., and Cornelis, G. R. (2002) *Infect. Immun.* **70,** 4165–4176
19. Dukuzumuremyi, J. M., Rosqvist, R., Hallberg, B., Akerstrom, B., Wolf-Watz, H., and Schesser, K. (2000) *J. Biol. Chem.* **275,** 35281–35290
20. Barz, C., Abahji, T. N., Trulzsch, K., and Heesemann, J. (2000) *FEBS Lett.* **482,** 139–143
21. Prehna, G., Ivanov, M. I., Bliska, J. B., and Stebbins, C. (2006) *Cell* **126,** 869–880
22. Juris, S. J., Rudolph, A. E., Huddler, D., Orth, K., and Dixon, J. E. (2000) *Proc. Natl. Acad. Sci. U. S. A.* **17,** 9431–9436
23. Wiley, D. J., Nordfeldth, R., Rosenzweig, J., DaFonseca, C. J., Gustin, R., Wolf-Watz, H., and Schesser, K. (2006) *Microb. Pathog.* **40,** 234–243
24. Spudich, J. A., and Watt, S. (1971) *J. Biol. Chem.* **246,** 4866–4871
25. Wegner, A. (1976) *J. Mol. Biol.* **108,** 139–150
26. Eichinger, L., Noegel, A. A., and Schleicher, M. (1991) *J. Cell Biol.* **112,** 665–676
27. Kouyama, T., and Mihashi, K. (1981) *Eur. J. Biochem.* **114,** 33–38
28. Heesemann, J., and Laufs, R. (1983) *J. Bacteriol.* **155,** 761–767
29. Bonaldi, T., Imhof, A., and Regula, J. T. (2004) *Proteomics* **4,** 1382–1396
30. Wiedemann, A., Linder, S., Grassl, G., Albert, M., Autenrieth, I., and Aepfelbacher, M. (2001) *Cell. Microbiol.* **10,** 693–702
31. Braun, V., Fraisier, V., Raposo, G., Hurbain, I., Sibarita, J. B., Chavrier, P., Galli, T., and Niedergang, F. (2004) *EMBO J.* **23,** 4166–4176
32. Roggenkamp, A., Neuberger, H. R., Flugel, A., Schmoll, T., and Heesemann, J. (1995) *Mol. Microbiol.* **16,** 1207–1219
33. Letzelter, M., Sorg, I., Mota, L. J., Meyer, S., Stalder, J., Feldman, M., Kuhn, M., Callebaut, I., and Cornelis, G. R. (2006) *EMBO J.* **25,** 3223–3233
34. Haugwitz, M., Noegel, A. A., Karakesisoglou, J., and Schleicher, M. (1994) *Cell* **79,** 303–314
35. Viboud, G. I., and Bliska, J. B. (2001) *EMBO J.* **20,** 5373–5382
36. Juris, S. J., Shah, K., Shokat, K., Dixon, J. E., and Vacratsis, P. O. (2006) *FEBS Lett.* **580,** 179–183
37. Soares, L., Seroogy, C., Skrenta, H., Anandasabapathy, N., Lovelace, P., Chung, C. D., Engleman, E., and Fathman, C. G. (2004) *Nat. Immunol.* **1,** 45–54